Studies of fracture in shear of a constrained layer

Ulf Stigh, Anders Biel

ulf.stigh@his.se

Abstract

Cracks normally propagate in the opening mode associated with a state of local symmetry at a crack tip. However, the micro- or macrostructure of a material or structure sometimes forces cracks to propagate in a shearing mode. Irrespective of the actual material studied, fracture in shear is frequently associated with the formation of a large number smaller sigmoidal-shaped cracks in the propagation direction of the major crack. Propagation of the major shear crack is accomplished by coalescing the sigmoidal-shaped cracks. Experiments show that the formation of sigmoidal cracks due to shear loading leads to a normal separation of the joined substrates. Theoretical studies show that constraining the local opening of the sigmoidal cracks increases the fracture resistance for the propagation of the major crack. In the present study, experiments with a ductile adhesive loaded in shear and where the normal separation is constrained are presented. The experiments are evaluated using the path independent J-integral. The associated cohesive law shows that considerable normal compressive stress develops in the adhesive during macroscopic shear loading. It is also concluded that by ignoring the normal separation in the evaluation of the experiments, the strength of the adhesive is underestimated. Thus, the procedure developed in earlier studies is conservative from a strength analysis perspective. The present technique might be possible to extend to other materials to reveal their properties in shear fracture

1 Introduction

Cracks are observed to propagate in shear under special circumstances, cf. e.g. [1]. Two different crack propagation mechanisms are observed on a smaller length scale: For some ductile materials, fibrils form and governs the fracture process through the stretching of the fibrils. In other materials, the shear crack is observed to be governed by a process of nucleation, growth and coalesce of smaller cracks, cf. e.g. [2]. These minor cracks appear to propagate in a state of local symmetry, i.e. with crack faces opening in the direction of the maximum tensile principal stress. In pure shear, in 45° relative to the direction of propagation of the major shear crack. If any of the minor cracks is not inhibited to grow in this direction, it will take over the role as the major crack and crack kinking occurs. However, if stiffer layers of material inhibit the propagation, the minor cracks form sigmoidal shapes in a shear

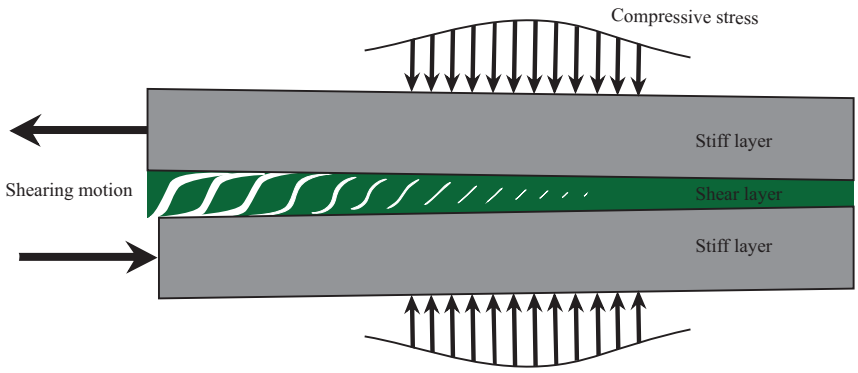

Figure 1: Shear crack propagation by nucleation, growth and coalesce of shear hackles. A shear crack propagates from left to right in this sketch of the fracture process. The shear hackles open up at the left due to their expansion.

layer, cf. Fig. 1. These are known as Riedels in soils, clay and rock, [3], shear hackles in composite materials, [4] and adhesive layers, [5].
During the fracture process, the shear hackles open-up and thus induce an expansion of the layer in which the shear crack propagates. The expansion increases during the fracture process and reaches a maximum at the tip of the growing shear crack. Far from the shear crack-tip, the fracture process is not initiated and the layer is not expanded. Thus, the expansion varies from a maximum at the shear crack-tip to a minimum far from the tip. This indicates that the constraints of the surrounding material influence the amount of expansion. With a soft surrounding, the expansion is expected to be large and with a stiff surrounding, the expansion is small. Due to the expansion of the surrounding material, a compressive stress is expected to act on the layer with shear hackles. Energetically, this means that part of the work performed to shear the layer is consumed to expand the surrounding material. From this, it can be expected that the work needed to fracture the layer in shear should increase as the stiffness of the surrounding material increases since more energy is needed to expand the layer. The shear layer also has to perform work against any source of compressive stress that acts over the layer. Thus, a compressive stress acting to close the shear hackles is expected to increase the work needed to fracture the layer, i.e. the apparent fracture energy. Thus, some care has to be exercised in measuring the fracture energy in shear J_{IIc} or J_{IIIc}, cf. [9].
In many materials showing this fracture process, the geometrical sizes and load levels are extreme. In polymeric adhesive layers, the mechanism can be studied experimentally under reasonable conditions. Appropriately designed and loaded specimens can force a major crack in the adhesive to propagate in a shearing mode at a reasonable load level and in a stable manner, cf. [6]. The findings from studies of shear fracture in adhesive layers is expected to be useful as an initial outset for studies of shear fracture in other materials.
A theoretical study shows the influence of constraining the expansion an elastic-brittle layer, cf. [7]. The study is based on linear elastic fracture mechanics and the principle of local symmetry. It shows that the work needed to fracture a brittle layer in shear is about 35% larger if the constraint is completely inhibited. Experimental studies indicate this effect for engineering adhesives. For tough adhesives, a more

constrained experimental set-up gives about 30% increased fracture energy, [8], and by actively constraining the expansion, the fracture energy increases by about 50%, [9].
By the expansion, there is no direct contact between the crack faces in the wake of a shear crack-tip. This means that Coulomb friction is not expected to play a major role in the fracture process. However, some distance from the crack tip, the crack faces may come into contact due to compressive loads and this may play an important role in a structural fracture process. Estimates of the effect are given in [10] and [11].
In the present paper a summary is given of some recent studies of shear fracture of structural adhesive layers. The next section introduces the method based on the path independent J-integral to be used to connect the shear fracture process to the external loads on test specimens. A cohesive zone model is used to quantify the shear properties of the shearing layer. It should be noted that no assumption on the shape of the cohesive law is assumed, it is only assumed that the same cohesive law governs the behaviour of the entire layer. The shape is a direct result from the experiments. The third section gives design guidelines for experimental methods to measure cohesive laws; especially for shear. Some experimental results are given in section 4 and the paper ends with a discussion and some conclusions.

2 Theory

The theoretical foundation is based on the path-independent J-integral given by

$$J = \int_S \left(U \mathrm{d}y + T_i u_{i,x} \mathrm{d}S \right), \tag{1}$$

in a planar state in the $x-y$-plane where no variation of the fields is allowed in the z-direction. The counter clockwise integration path is denoted S; $\mathbf{T}$ and $\mathbf{u}$ are the traction vector acting on the interior of S, and the displacement vector, respectively; U is the strain energy density, cf. [12] and [13]. Index notation is used with Einstein's summation convention and a comma indicating partial differentiation. If the material is homogeneous in the x-direction, i.e. if U is not explicitly dependent of x, the integral is path independent. This can be shown by evaluating the integral for a *closed* path S not surrounding any object that would change the potential energy if the object is moved in the x-direction. With the help of the divergence theorem, $J = 0$ results. Moreover, the integral gives the configurational force on any object residing inside S, [14]. From these results two conjectures can be drawn: 1) the integration path S can be chosen arbitrarily and Eq. (1) gives the same configurational force as long as S contains the same energy-changing objects and 2) the sum of J for all energy-changing objects in an elastic field is zero. Thus, the configurational forces are in equilibrium in the same way as ordinary forces are in equilibrium, cf. e.g. [15]. These results are useful in the design of test specimens to measure cohesive laws.
Equation (1) is based on the existence of a strain energy density U. This appears as a serious limitation of the applicability of the integral. However, as long as no

unloading takes place, a pseudopotential can take the place of U. That is, the stress can formally be derived by differentiating U with respect to the strain. By this, the applicability of the J-integral is extended to inelasticity when no unloading takes place.
A cohesive zone located in a plane $y = \text{constant}$[1] is governed by a cohesive law,

$$\sigma = \frac{\partial \bar{J}}{\partial w} \tag{2}$$

$$\tau = \frac{\partial \bar{J}}{\partial v} \tag{3}$$

where $\bar{J}$ is a potential for the cohesive normal stress σ in the y-direction, positive when opening the cohesive zone, and the cohesive shear stress τ in the $x-$direction. The conjugated separations are w in the y-direction, denoting the opening and v in the x-direction, denoting the shear. A direct application of Eq. (1) shows that $\bar{J} = J$. This result is derived in [13] for pure opening and it is readily extended to a mixed loading giving Eqs. (2) and (3). An alternative derivation is given in [16].

3 Design of specimen

The energy changing objects identified in test-specimens are boundaries and loading points. Taking the x-axis horizontally, and choosing S to closely encircle a traction free boundary, Eq. (1) shows that a free horizontal boundary does not contribute to J. Similarly, a stress free vertical boundary does not contribute to J. Practically, this can often be achieved by allowing for some overhang at loading points and supports.
Any horizontal boundary between different materials, i.e. a jump in U in the y-direction, does not contribute to J. This is shown by considering that the first term in the integrand of Eq. (1) does not contribute if S is chosen to follow the interface closely on each side. The second term does not contribute either. This follows from the continuity properties of $\mathbf{T}$ and $\mathbf{u}$, cf. [17].
A vertical force P acting on an otherwise free horizontal boundary contributes with J_{P} to J. This is shown by applying Eq. (1) to the boundary.

$$J_{\mathrm{P}} = \frac{P\theta}{b} \tag{4}$$

Here θ is the rotation of the loading point and b is the out-of-plane width of the specimen, cf. [16].
These results are applied to the modified end notched flexure (ENF) specimen, cf. Fig. 2. The specimen consists of two steel bars, i.e. the substrates, and an adhesive layer terminated the distance a from the left support. In an ordinary ENF-specimen, the loading F, Δ is applied at the centre between the supports. By

[1] It can be helpful to consider Fig. 1 with a horizontal x-axis directed to the right and a vertical y-axis directed upwards.

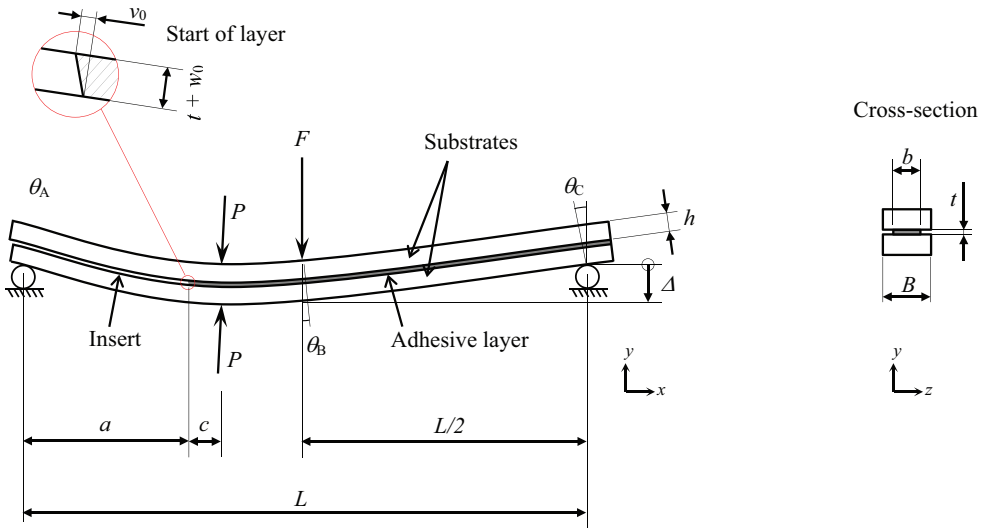

Figure 2: Deformed modified end notched flexure specimen.

gradually increasing the prescribed deflection Δ, the fracture process is initiated at the left end of the layer and eventually a shear crack is formed. The process is stable if the length a is long enough. For a brittle layer, the condition is $a/L > 0.35$ and a somewhat shorter a can be chosen if the layer is tough, cf. [6]. Here, the specimen is modified by a pair of forces P applied close to the left end of the layer, the distance c in Fig. 2. These forces limit the expansion of the shearing layer. In an experiment, P is applied first and kept constant thereafter Δ is gradually increased.

4 Experiments and results

Experiments with the rubber based commercial structural adhesive DowBetamate-5096 are presented in [16]. A brief summary is given here. Cohesive laws are unique for a specific layer thickness. In this study the thickness $t = 0.3$ mm. Two different crack lengths are used $a = 300$ and 350 mm, respectively. The substrates are made of tool steel with a distance L =1 m between the supports. Non of the experiments suffers inelastic deformation of the substrates or instability of crack propagation although the shorter a violates the stability condition for brittle adhesives in [6]. The experiments are performed quasistatically at a loading rate $\dot{\Delta} = 2$ mm/min in a servo hydraulic testing machine (Instron 8802). It is expected that the loading rate influences the evaluated data, cf. e.g. [18]. During the experiments, the expansion w_0 and the shear v_0 at the crack tip are measured using LVDTs. Repeated experiments are performed at five different values of the constraining force $P = 0$, 1.25, 2.50, 3.75, and 5.00 kN.

Figure 3 shows J vs. v and w_0 vs. v_0, respectively with $P = 5$ kN. Although two different specimen geometries are used, i.e. $a = 300$ and 350 mm, there is no sign of this difference in the evaluated data. This supports that the evaluation procedure gives data for the *layer* and not for the specimen, as expected. The red curves are least square adaptions to the experimental data.

The J-curves show a parabolic shape for small v indicating a linear elastic response

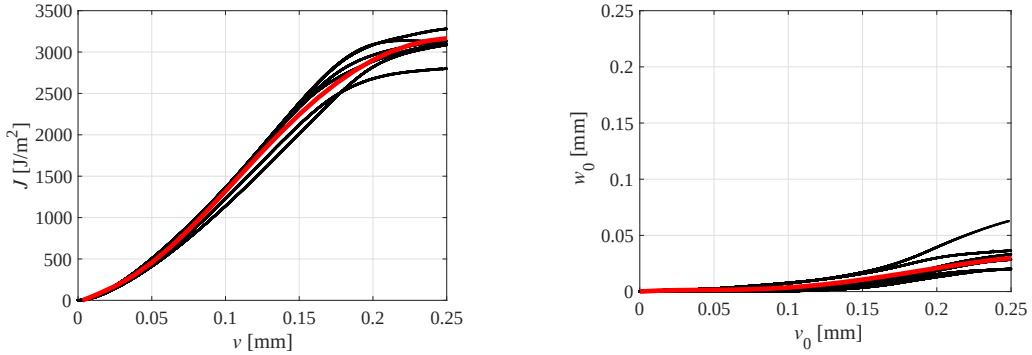

(a) (b)

Figure 3: a) Evaluated J vs. v and b) measured w_0 vs. v_0 for $P = 5$ kN. Black curves: experimental data; red curves: adapted curve. Data from [16]. Note that the $J - v$-relation is assumed to be the same for the entire layer, i.e. the index 0 is dropped on v in the left graph.

for small deformation. This part ends at $v \approx 0.035$ mm irrespective of the level of constraining force P. The shape of the next section of the J-curves corresponds approximately to a cohesive law with linear hardening plasticity. This phase ends when the expansion w_0 becomes considerable. With a larger P this occurs later in the loading history. After this, J continues to increase but with a negative second derivative corresponding to a softening cohesive law, cf. Eq. (3). At $w \approx 0.25$ mm, the J-curve levels out corresponding to zero shear stress and a shear crack has formed.

The w_0 vs. v_0 curves in Fig. 3b shows that the expansion is considerable at fracture even at $P = 5$ kN which is the maximum constraining force in the experimental series, cf. [16]. To derive a cohesive law for pure shear, i.e. for $w = 0$, an extrapolation method is needed. The following procedure is developed in [16]. For 20 consecutive values of v, values of J and w are derived from the adapted J vs. v curves and the w_0 vs. v_0 curves exemplified in Fig. 3. Lines are adapted to the J and w data for each value of v. Each line is extrapolated to $w = 0$ giving a value of J. This gives 20 values of J vs. v for pure shear, i.e. $w = 0$. Figure 4a shows the result. It shows a maximum at $J_{\mathrm{IIc}} = 3.2$ kN/m, i.e. the fracture energy is considerably larger in pure shear than the value 2.1 kN/m evaluated from the experimental series with $P = 0$, cf. [16].

The black curve is a least square adaption. Differentiation of this according to Eq. (3) gives the cohesive law $\tau(v)$ in Fig. 4b. The cohesive shear strength is $\hat{\tau} = 22$ MPa. This is also larger than the value derived from the experiments with $P = 0$ if they are evaluated by ignoring the expansion. This erroneous evolution yields the shear strength 16 MPa. Thus, ignoring the expansion of the layer in the evaluation yields smaller values of the fracture energy and cohesive strength.

The extrapolation procedure also provides an evaluation of the cohesive normal stress for pure shear deformation. The slope of each of the 20 lines adapted to the J vs. w data, is the corresponding normal stress according to Eq. (2). The result is shown as circles in Fig. 4b. A considerable compressive stress develops in

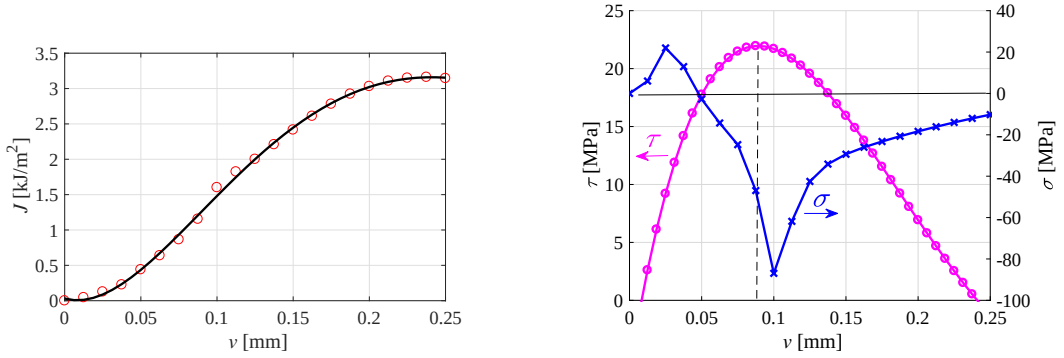

(a) (b)

Figure 4: a) Derived J vs. v for pure shear, i.e. $w = 0$. Circles: extrapolated data; black curve: least square adaption. b) Cohesive law for pure shear. Purple curve: Shear stress vs. shear; Blue curve: Normal stress vs. shear. Data from [16].

conjunction with the formation of the shear hackles, i.e. $\sigma \approx$ -85 MPa at $v = 0.1$ mm. When the shear hackles grow, the layer becomes less stiff in compression, and the compressive stress decreases. However, some compressive stress remain when the shear crack has formed at $v \approx 0.25$ mm. This can be a result of debris of the layer left in the wake of a propagating crack and supporting normal stress.
The positive normal stress derived at small values of v can be an artefact of the extrapolation procedure. As shown in Fig. 3b, w_0 develops very slowly with v_0 at the start of an experiment. This results in large relative deviations between the data and the adapted curves for small values of v, i.e. for $v \lesssim 0.05$ mm. As discussed above, it is expected that the layer responds elastically for $|v| \lesssim 0.035$ mm. As the elastic response must be derived from a strain potential to satisfy basic thermodynamics, and since $\tau = 0$ is the only possibility for $v = 0$ and $w > 0$, $\sigma = 0$ is the only possibility for $w = 0$ and $v > 0$ due to the symmetry of the elastic stiffness matrix resulting from the existence of a potential. Thus, the positive σ for $v \lesssim 0.035$ mm in Fig. 4b is most likely an artefact of errors developed in the extrapolation procedure for small v, cf. [16].

5 Discussion and conclusions

Normally, materials do not fracture in shear. Without a layered structure confining crack propagation to shear, as in the cases of composite materials and adhesive joints, or due to a considerable compressive stress, as is the case in tectonic plates, crack kinking occurs. Cracks prefer mode I, cf. e.g. [1]. In many cases of shear fracture, shear hackles develop during the fracture process. These force the crack tip to open up, i.e. crack opening occurs even if the external loads and the geometry suggest a state of pure shear. This un-symmetry is given by the material behaviour. Since crack opening occurs, friction cannot develop in the close vicinity of the crack-tip. Friction can however develop some distance from the crack tip if large compressive loads act.
The experimental method developed in [9] and the evaluation procedure developed

in [16] yield data for a cohesive zone model of a thin layer fracturing in shear by the development of shear hackles. A modified ENF-specimen is used and evaluated based on the path- independent properties of the J-integral. After extrapolation of the experimental data to a state of pure shear deformation, the cohesive laws for shear stress vs. shear and normal stress vs. shear are derived. The results show larger fracture energy and strength than evaluated by ignoring the expansion. This indicates that earlier results ignoring this expansion are conservative in a design situation; they underestimate the cohesive strength and fracture energy of the adhesive layer.
The effect of constraining the expansion is larger than expected from a theoretical analysis, cf. [7] and [16]. This is attributed to the considerable toughness of the adhesive that invalidates a direct analysis based on linear elastic fracture mechanics. Thus, it is indicated that toughness increases the effect of constraining the expansion. From a designers point of view, it is interesting to note that different engineering methods to improve joints and composites by e.g. adding mechanical fasteners such as rivets in adhesive joints or stitching the layers together in composite materials have an unexpected effect to improve the shear strength by constraining the expansion.
The mechanism presented here might shed some light on the size-effect of the delamination strength noted in e.g. [19].

Acknowledgements

The authors are grateful to the Knowledge foundation for financial support for part of this study.

References

[1] K.B. Broberg. Cracks and fracture. Academic Press, San Diego, 1999

[2] U. Stigh, A. Biel, T. Walander. Shear strength of adhesive layers - Models and experiments. Engineering Fracture Mechanics. 129:67-76, 2014.

[3] W. Riedel. Zur mechanik geologischer brucherscheinungen. Zentralblatt für Mineral, Geologie und Paläontologie, 354-368, 1929.

[4] M.D. Gilchrist, N. Svensson. A fractographic analysis of delamination within multidirectional carbon/epoxy laminates. Composites Science and Technology, 55:195-207, 1995.

[5] H. Chai. Shear fracture. International Journal of Fracture, 37:137-159, 1988.

[6] K.S. Alfredsson, U. Stigh. Stability of beam-like fracture mechanics specimens. Engineering Fracture Mechanics, 89:98-113, 2012.

[7] Z.C. Xia, J.W. Hutchinson. Mode II fracture toughness of a brittle adhesive layer. International Journal of Solids Structures, 31:1133-1148, 1994.

[8] F.A. Leone Jr, D. Girolamo, C.G. Dàvila. Progressive damage analysis of bonded composite joints. NASA/TM-2012-217790, 2012.

[9] U. Stigh, A. Biel. Shear properties of an adhesive layer exposed to a compressive load. Procedia Materials Science. 3:1626-1631, 2014.

[10] L.A. Carlsson, J.W. Gillespie Jr, R.B. Pipes. On the analysis and design of the end notched flexure (ENF) specimen for mode II testing. Journal of Composite Materials, 20:594-604, 1986.

[11] C. Fan, P.-Y. Ben Jar, J.-J.Roger Chen. A unified approach to quantify the role of friction in beam-type specimens for the measurement of mode II delamination resistance of fibre-reinforced polymers. Composites Science and Technology 67 (2007) 989-995.

[12] G.P. Cherepanov. The propagation of cracks in a continuous medium. Journal of Applied Mathematics and Mechanics, 31(3):503-512, 1967.

[13] J.R. Rice. A path independent integral and the approximative analysis of strain concentration by notches and cracks. ASME Journal of Applied Mechanics, 88:379-386, 1968.

[14] J.D. Eshelby. The force on an elastic singularity. Philosophical Transactions of the Royal Society of London A244:87-112, 1951.

[15] D. Svensson, K.S. Alfredsson, U. Stigh, N. Jansson. Measurement of cohesive law for kink-band formation in unidirectional composite. Engineering Fracture Mechanics 151:1-10, 2016.

[16] A. Biel, U. Stigh. Strength and toughness in pure shear of constrained layers. Submitted.

[17] U. Stigh. Applications of equilibrium of configurational forces for the measurement of cohesive laws. Proceedings of the 17th European conference on composite materials, Münich 2016.

[18] T. Carlberger , A. Biel, U. Stigh. Influence of temperature and strain rate on cohesive properties of a structural epoxy adhesive. International Journal of Fracture 155:155-166, 2009.

[19] M.R. Wisnom. On the increase in fracture energy with thickness in delamination of unidirectional glass fibre-epoxy with cut central plies. Journal of Reinforced Plastics and Composites, 2:897-909, 1992.

Ulf Stigh, University of Skövde, Sweden
Anders Biel, University of Skövde, Sweden